Two-photon microscopy by wavelength-swept pulses delivered through single-mode fiber

Jeon Woong Kang,[1] Pilhan Kim,[1] Carlo Amadeo Alonzo,[1] Hyunsung Park,[1,2] and Seok H. Yun[1,2,*]

[1]*Harvard Medical School and Wellman Center for Photomedicine, Massachusetts General Hospital, 50 Blossom Street, BAR-8, Boston, Massachusetts 02114, USA*

[2]*Graduate School of Nanoscience and Technology and WCU Program, KAIST, 335 Gwahak-ro, Yuseong-gu, Daejeon 305-701, Korea*

**Corresponding author: syun@hms.harvard.edu*

Received September 16, 2009; revised November 30, 2009; accepted December 3, 2009; posted December 10, 2009 (Doc. ID 117297); published January 13, 2010

Nonlinear microscopy through flexible fiber-optic catheters has potential in clinical diagnostic applications. Here, we demonstrate a new approach based on wavelength-swept narrowband pulses that permits simple fiber-optic delivery without need of the dispersion management and allows nonmechanical beam scanning. Using 0.86 ps pulses rapidly tuned from 789 nm to 822 nm at a sweep rate of 200 Hz, we demonstrate two-photon fluorescence and second-harmonic generation imaging through a 5-m-long standard single-mode fiber. © 2010 Optical Society of America

OCIS codes: 110.0180, 140.3600, 180.4315.

Since its introduction in 1990, two-photon fluorescence microscopy has become a powerful tool to visualize biological processes in live specimens [1]. Although this technique has been extensively applied to research, it also has promising potential in clinical applications. Useful pathologic and physiologic information can be obtained *in vivo* by direct visualization of various endogenous molecules and extracellular matrix [2]. However, owing to limited optical penetration in tissue, realizing this potential in the clinic requires a minimally invasive instrument capable of accessing remote locations within the body via flexible, small-diameter endoscopes or catheters.

A standard two-photon microscope employs a pulsed laser source and a rapid beam scanner. One approach to flexible endoscopy involves delivering the excitation pulses through an optical fiber and scanning the beam with a miniature scanner integrated in the distal end of the probe [3]. This instrumentation of endoscopy, although actively exploited, presents a number of technical challenges. Mode-locked solid-state lasers are typically used to provide pulse widths of about 100 fs and pulse energies in the order of 1 nJ into the imaging system. The resulting high peak power, about 10 kW, makes it difficult to deliver these pulses through conventional single-mode fibers (SMFs) without serious pulse broadening caused by self-phase modulation and group-velocity dispersion [4]. To overcome this problem, researchers have used specialty fibers, such as hollow-core photonic bandgap fibers [5] and large-mode-area fibers [6], but they are not readily compatible with standard optical components and are much more expensive than standard SMF. Prepulse and postpulse chirping have been proposed to mitigate the nonlinear distortion in standard SMF [7]. However, this scheme adds complexity and works best with a relatively short, predetermined, fiber length. Furthermore, because of strong chromatic dispersion of silica at wavelengths below 1 μm, it is nontrivial to transmit even low-energy pulses over several meters of standard SMF. Fast beam scanning required for real-time imaging represents another challenge. Mechanical scanners, such as resonant piezotransducers [8] and microelectricalmechanical system actuators [9], have been continuously improved. However, two-axis video-rate scanning with a form factor less than a few millimeters in diameter remains particularly difficult.

Spectral encoding is a nonmechanical scanning method that uses a dispersive element, such as a diffraction grating, to convert the spectrum to a spatial distribution along a transverse line [10]. This scanning mechanism can replace a fast-axis mechanical scanner and therefore facilitate development of miniature fiber-optic endoscopes. Spectrally encoded imaging has been demonstrated for confocal reflectance microscopy using spectrometers [11] or wavelength-swept lasers [12]. The feasibility of spectral encoding in two-photon microscopy has also been demonstrated by using a manually tunable laser and free-space configuration [13].

Here, we report fiber-optic two-photon microscopy using rapidly tuned, spectral encoding laser pulses delivered through standard SMF. We show that the relatively narrow spectral width of individual pulses allows flexible delivery over several meters of SMF without significant degradation of nonlinear excitation efficiency. Using a fiber-optic bench-top system, we demonstrate the feasibility of real-time two-photon fluorescence and second-harmonic-generation (SHG) imaging without need for rapid mechanical scanning.

Consider a series of short optical pulses with center wavelengths varying continuously from pulse to pulse, as illustrated in Fig. 1(a). When this pulse train encounters a diffraction grating, the propagation direction of each pulse is altered according to its respective center wavelength, resulting in a lateral line scan after passing a focusing lens. Each point in the focal line is illuminated sequentially as the center wavelength is swept rapidly and repeatedly over time.

0146-9592/10/020181-3/$15.00

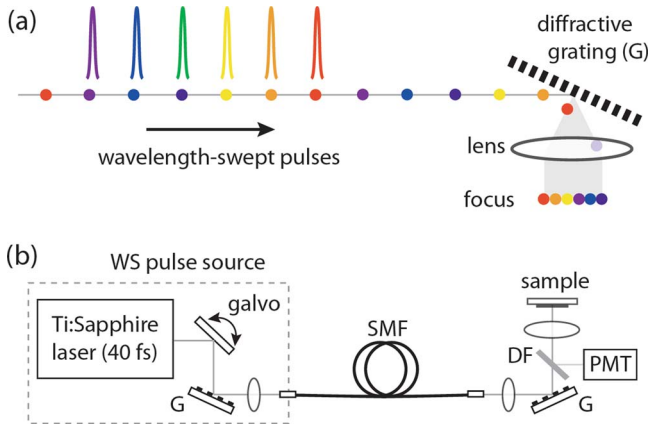

Fig. 1. (Color online) (a) Diffraction-based line scan of wavelength-swept pulses. (b) Schematic of the experimental setup.

We implemented this spectral encoding principle in a bench top setup shown in Fig. 1(b). To generate wavelength-swept pulses, we used a mode-locked Ti:sapphire laser (Del Mar Photonics, Trestle100) and transmitted its broadband output (λ_{FWHM} = 25 nm at 805 nm, 300 mW, 93 MHz) through an external tunable filter consisting of a galvanometer-mounted mirror (Cambridge Technology) and a diffraction grating (830 g/mm). The core of an SMF (Thorlabs, P3-830A-FC-5, 5 m), serving as a pinhole, receives and transmits only a specific spectral component corresponding to the voltage applied to the galvanometer. By applying a modulation signal, the center wavelength of the filter is tuned continuously at a repetition rates up to a few kilohertz. Higher tuning rate beyond 100 kHz would be possible if a faster scanning element, such as a spinning polygon or resonant Fabry–Perot etalon, is used instead of the galvanometer. We designed the filter to have a 3 dB bandwidth of 1.1 nm and a tuning range of 33 nm across the input laser spectrum, yielding 30 resolvable points (N). External filtering is simple but inevitably involves significant power loss compared to intracavity tuning [14]. We obtained average power of 3 mW at the output end of the SMF.

The output beam from the fiber was collimated by an aspheric lens, which we chose to maintain the same number of resolvable points (N=30) after the second grating (300 g/mm) and also to fill the aperture of an aspheric objective lens (Thorlabs, C330TME-B, f=3.1 mm). From this arrangement and with the 33 nm spectral range, we achieved a field of view (line) of about 30 μm. The signal light reemitted from a sample is reflected by a dichroic mirror, transmitted through bandpass filters, and detected by a photomultiplier tube. Notably, remote fiber-optic detection is also feasible, but we did not implement such a configuration in our proof-of-concept experiments. To produce 2D images, we used a motorized stage to move the sample along the slow axis orthogonal to the spectrally encoded fast axis. A 12-bit data acquisition board was used to control the galvanometer, motorized stage, digitization, and image display in real time.

Figure 2(a) shows the peak-hold output spectrum, measured with an optical spectrum analyzer (Agilent, 86142B), of the sweeping source measured when driven with a saw-tooth voltage signal at a frequency of 200 Hz. For comparison, we also plotted several representative narrowband spectra, each of which was obtained at a constant voltage to the galvanometer. The optical bandwidth of each spectrum was measured to be 1.1 nm as designed, which corresponds to a temporal width of 0.86 ps for transform-limited Gaussian pulses. Figure 2(b) depicts an oscilloscope trace of the sweeping source output (cyan curve), measured with a silicon receiver.

We used the swept laser output to generate fluorescence from rhodamine B solution (2 mg/ml). The square root of fluorescence signal measured by the photomultiplier tube showed an excellent correlation with the illumination power, as depicted in Fig. 2(b). This quadratic dependence confirms two-photon absorption. The correlation indicates that the propagation over the 5-m-long SMF caused insignificant ($<$10%) nonlinear broadening. Indeed, in computer simulation we verified near-penalty-free delivery. We also performed the same experiment using femtosecond pulses (25 nm, ~40 fs) from the Ti:sapphire laser without external filtering and measured much weaker fluorescence signal compared with the narrowband (1.1 nm) pulses at the same delivered power (3 mW). We attributed the signal degradation to temporal broadening of the femtosecond pulses in the SMF. It is well known that two-photon signal is inversely proportional to the pulse width. In fact, without pulse broadening, 40 fs pulses should produce fluorescence ~20 times stronger than from picosecond pulses of equivalent average power, as we confirmed in a free-space experiment.

In SMF, group velocity dispersion (GVD) and self phase modulation (SPM) each contribute to pulse broadening. While broadening generally scales with propagation distance, the influence of GVD and SPM vary inversely with the square of pulse width and directly with the pulse peak power. Thus, if average power is held constant, both broadening effects are stronger for narrower pulses. Our numerical simulations showed that, consistent with the experimental

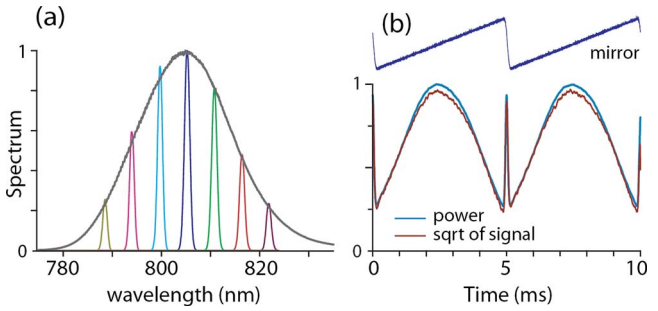

Fig. 2. (Color online) (a) Peak-hold spectral envelope (black) of rapidly swept pulses, and individual spectra measured with the narrowband filter fixed at specific wavelengths. (b) Temporal trace of the square root of two-photon signal (dark gray), overlaid with the intensity envelope of sweeping source (light gray). Also shown is the galvanometer position signal (black).

results, GVD and SPM had little effect on the two-photon signal of a 0.9 ps pulse at 3 mW average power [Figs. 3(a) and 3(b)]. In contrast, a 45 fs pulse at the same center wavelength underwent rapid broadening mainly because of GVD; after 5 m of SMF, two-photon signal dropped to 0.4% compared to an equivalent free-space propagated pulse [Figs. 3(c) and 3(d)]. This is far below the initial factor-of-20 deficit of the picosecond pulse and demonstrates how picosecond pulses are advantageous over femtosecond pulses in two-photon imaging through several meters of standard SMF, even at modest power levels.

Using the wavelength-swept source driven at 200 Hz, we performed fluorescence imaging of a lens cleaning tissue stained with a drop of rhodamine B solution (2 mg/1 ml). Figure 4(a) shows a representative image of the dried sample, showing individual stained tissue fibers. The pixels in horizontal axis correspond to different excitation wavelengths. The nonuniform laser power across the spectrum resulted in the variation of signal generation efficiency across this axis, as evident in Fig. 2. To minimize the resulting image artifact, we normalized each pixel value with the corresponding square of excitation intensity. Synchronized with the wavelength scan, the sample on the motorized stage was translated with 1 μm steps along the slow (vertical) axis. Figure 4(b) shows a mosaic image produced by stacking multiple images. We also imaged fresh murine tail tendon via SHG. For SHG detection, we used a 60 nm bandpass filter centered at 417 nm. Figure 4(c) shows a mosaic image spanning 150 μm by 150 μm. It clearly visualizes the typical wavy fiber structure aligned parallel to the longitudinal axis [2].

In conclusion, we have demonstrated a novel technique for fiber-optic two-photon microscopy. We showed that the use of rapidly swept narrowband pulses could facilitate fiber-optic delivery and simplify beam scanning. With appropriate intracavity tuning of a Ti:sapphire laser, it should be possible to generate picosecond swept pulses over a range wider than 150 nm, providing more than 100 resolvable points. The technique we presented may be well suited for clinical diagnostic imaging, in particular, through rotating catheters [15], to examine gastrointestinal tracts, respiratory airways, and coronary arteries.

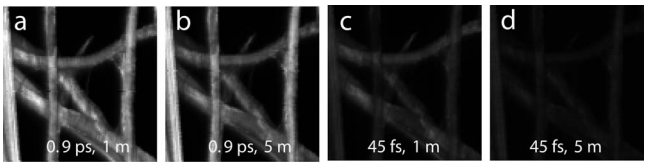

Fig. 3. Comparison of two-photon fluorescence generation efficiency for various pulse widths and propagation lengths over SMF: a, 0.9 ps, 1 m fiber delivery; d, 0.9 ps, 5 m; c, 45 fs, 1 m; b, 45 fs, 5 m. Images show a paper tissue stained with rhodamine B.

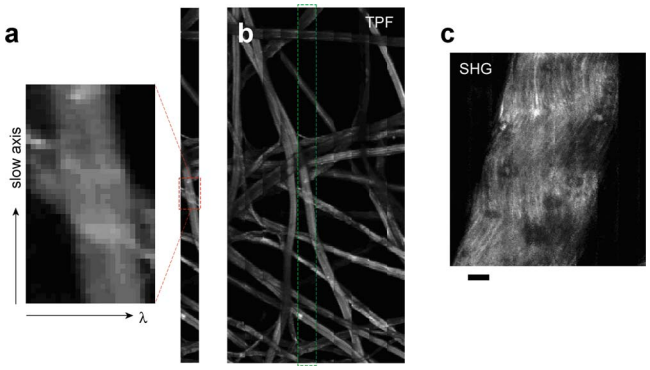

Fig. 4. (Color online) Two-photon imaging by wavelength-swept picosecond pulses. a, Fluorescence image of lens tissue stained with rhodamine B. The horizontal line scan rate is 200 Hz, determined by the wavelength sweep rate. b, Mosaic image of the lens tissue. c, Second-harmonic-generation mosaic image of murine tail tendon. Scale bar, 30 μm.

The authors acknowledge the support by the National Science Foundation (NSF) (ECCS-0801412), the National Research Foundation of Korea (R31-2008-000-10071-0 and fellowship KRF-2007-357-C00036 to J. W. K.), and Human Frontier Science Program (Cross Disciplinary Fellowship to P. K.).

References

1. W. Denk, J. H. Strickler, and W. W. Webb, Science **248**, 73 (1990).
2. W. R. Zipfel, R. M. Williams, R. Christie, A. Y. Nikitin, B. T. Hyman, and W. W. Webb, Proc. Natl. Acad. Sci. U.S.A. **100**, 7075 (2003).
3. D. Bird and M. Gu, Opt. Lett. **28**, 1552 (2003).
4. G. P. Agrawal, *Nonlinear Fiber Optics* (Academic, 2001).
5. W. Göbel, A. Nimmerjahn, and F. Helmchen, Opt. Lett. **29**, 1285 (2004).
6. S. Ramachandran, M. F. Yan, J. Jasapara, P. Wisk, S. Ghalmi, E. Monberg, and F. V. Dimarcello, Opt. Lett. **30**, 3225 (2005).
7. A. M. Larson and A. T. Yeh, Opt. Express **16**, 14723 (2008).
8. M. T. Myaing, D. J. MacDonald, and X. Li, Opt. Lett. **31**, 1076 (2006).
9. W. Piyawattanametha, E. D. Cocker, L. D. Burns, R. P. J. Barretto, J. C. Jung, H. Ra, O. Solgaard, and M. J. Schnitzer, Opt. Lett. **34**, 2309 (2009).
10. G. J. Tearney, R. H. Webb, and B. E. Bouma, Opt. Lett. **23**, 1152 (1998).
11. D. Yelin, C. Boudoux, B. E. Bouma, and G. J. Tearney, Opt. Lett. **32**, 1102 (2007).
12. C. Boudoux, S. H. Yun, W. Y. Oh, W. M. White, N. V. Iftimia, M. Shishkov, B. E. Bouma, and G. J. Tearney, Opt. Express **13**, 8214 (2005).
13. K. Shi, S. Yin, and Z. Liu, J. Microsc. **223**, 83 (2006).
14. S. H. Yun, Opt. Lett. **30**, 2660 (2005).
15. S. H. Yun, G. J. Tearney, B. J. Vakoc, M. Shishkov, W. Y. Oh, A. E. Desjardins, M. J. Suter, R. C. Chan, J. A. Evans, I. Jang, N. S. Nishioka, J. F. de Boer, and B. E. Bouma, Nat. Med. **12**, 1429 (2006).